1.0

1.1

1.25   1.4   1.6

4.5
5.0
5.6
6.3

2.8   2.5

3.2   2.2

3.6

4.0   2.0

1.8

MICROCOPY RESOLUTION TEST CHART
NATIONAL BUREAU OF STANDARDS-1963-A

REPORT DOCUMENTATION PAGE

READ INSTRUCTIONS
BEFORE COMPLETING FORM

1. REPORT NUMBER	2. GOVT ACCESSION NO.	3. RECIPIENT'S CATALOG NUMBER
N00014-76-C-0727-4		

4. TITLE (and Subtitle)

PHASE TRANSITIONS IN THE CHEMISORBED LAYER W(110)p(2x1)-O AS A FUNCTION OF COVERAGE: I. EXPERIMENTAL.

5. TYPE OF REPORT & PERIOD COVERED

Technical Report

6. PERFORMING ORG. REPORT NUMBER

7. AUTHOR(s)

G.-C. Wang, T.-M. Lu, & M.G. Lagally

8. CONTRACT OR GRANT NUMBER(s)

N00014-76-C-0727

9. PERFORMING ORGANIZATION NAME AND ADDRESS

Board of Regents of the University of Wisconsin System, 750 University Avenue, Madison, WI 53706

10. PROGRAM ELEMENT, PROJECT, TASK AREA & WORK UNIT NUMBERS

NR 392-014

11. CONTROLLING OFFICE NAME AND ADDRESS

Office of Naval Research
Arlington, VA 22217

12. REPORT DATE

December 77

13. NUMBER OF PAGES

30

14. MONITORING AGENCY NAME & ADDRESS(if different from Controlling Office)

Office of Naval Research
Branch Office Chicago
536 S. Clark St., Rm. 286
Chicago, Il 60605

15. SECURITY CLASS. (of this report)

Unclassified

15a. DECLASSIFICATION/DOWNGRADING SCHEDULE

16. DISTRIBUTION STATEMENT (of this Report)

Approved for public release; distribution unlimited.

17. DISTRIBUTION STATEMENT (of the abstract entered in Block 20, if different from Report)

D D C
JAN 24 1978
RECEIVED
F

18. SUPPLEMENTARY NOTES

Preprint, submitted to J. Chem. Phys.

19. KEY WORDS (Continue on reverse side if necessary and identify by block number)

Surfaces, chemisorbed layers, adatom-adatom interactions, phase transitions, low-energy electron diffraction.

20. ABSTRACT (Continue on reverse side if necessary and identify by block number)

The thermal disordering of oxygen chemisorbed on W(110) has been investigated as a function of coverage below half monolayer coverage by measuring the angular distribution of intensity in the LEED superlattice reflections as a function of temperature. The transition temperature is a function of coverage, being much lower at low coverage. A partial phase diagram is constructed for this overlayer, and the low- and high-coverage limits are interpreted respectively in terms of an island-dissolution and an order-disorder transition.

DD FORM 1473 EDITION OF 1 NOV 65 IS OBSOLETE
1 JAN 73
S/N 0102-014-6601

TECHNICAL REPORT

PHASE TRANSITIONS IN THE CHEMISORBED
LAYER W(110) p(2x1)-O AS A FUNCTION OF
COVERAGE: I. EXPERIMENTAL

by

G.-C. Wang, T.-M. Lu, & M.G. Lagally
Materials Science Center
University of Wisconsin
Madison, Wisconsin 53706

December 27, 1977

PHASE TRANSITIONS IN THE CHEMISORBED
LAYER W(110) p(2x1)-O AS A FUNCTION OF
COVERAGE: I. EXPERIMENTAL[†]

G.-C. Wang, T.-M. Lu, & M.G. Lagally[*]

Department of Metallurgical and Mineral Engineering
and Materials Science Center
University of Wisconsin
Madison, Wisconsin 53706

ABSTRACT

The thermal disordering of oxygen chemisorbed on W(110) has been
investigated as a function of coverage below half monolayer coverage
by measuring the angular distribution of intensity in the LEED super-
lattice reflections as a function of temperature. The transition
temperature is a function of coverage, being much lower at low coverage.
A partial phase diagram is constructed for this overlayer, and the
low- and high-coverage limits are interpreted respectively in terms
of an island-dissolution and an order-disorder transiton.

I. INTRODUCTION

When atoms or molecules adsorb on a crystalline surface, they undergo interactions not just with the substrate but with each other as well. That such interactions exist is, of course, easily demonstrated by the observation with low-energy electron diffraction (LEED) that ordered superlattices of adsorbate atoms form on crystalline substrates.[1] These interactions may be due mainly to dispersion forces, as for physisorbed layers,[2] or may be dominated by chemical interactions. Such interactions may be of particular importance in chemical reactions on surfaces, in that they may provide a rate-limiting step to a given reaction. Although considerable work, both theoretical and experimental, studying chemisorption exists, the understanding of adatom-adatom (A-A) interactions is still quite limited. Theoretically, some of the framework exists for including A-A interactions in chemisorption models.[3] Experimentally, a number of techniques have been applied to investigate the effect of A-A interactions, including isosteric heat measurements,[4] flash desorption,[5] field ion microscopy,[6] and measurement of phase changes in overlayers, both with temperature and coverage, by LEED.[7-12] The study of phase changes with temperature in chemisorbed overlayers, observed some time ago,[7] promises to be an important tool in obtaining a quantitative understanding of the interactions that adatoms undergo. However, few of the chemisorption systems studied only H on W(100)[8,13] and O on W(110)[10,14] have been analyzed in any detail.[14a] In both of these cases, measurements and analysis were limited to half-monolayer coverage, i.e., to saturation coverage for the particular overlayer structure that corresponds to one-half substrate site

occupancy by adatoms. These are denoted respectively as W(100) c(2x2)-H and

W(110)p(2x1)-0. In such cases, use of simple Bragg-Williams or Ising models

offered the possibility of approximating A-A interactions by fitting the

transition temperature.[8]

In chemisorption on single-crystal surfaces, it is known that of the

gas atoms (molecules) impinging randomly on the surface a certain fraction

at any coverage and gas and crystal temperatures (proportional to the

sticking coefficient under these conditions) becomes accommodated by

the substrate holding potential, and then by some surface diffusion mechanism these atoms

migrate either to condense in patches of particular order and symmetry

relative to the substrate or to assume a more or less random arrangement.

Which of these occurs under any conditions of coverage and temperature

depends on which state is the one of minimum free energy, which in turn

depends on the relative magnitude and sign of the adatom - adatom interactions.

For many adsorbates, ordered regions form at room temperature already

at much less than saturation coverage. This is demonstrated by the

observation of "sharp" LEED superlattice reflections at these low coverages.[1]

In fact, from such observations, the sign of A-A interactions in different

directions, for different coordination, and for different neighbors can

frequently be ascertained. Monte Carlo modeling of the ordering of an

assumed initially disordered adlayer of the proper density reproduces this

ordering if interactions of the proper sign (and any assumed magnitude) are

included in the model.[15] A basic result is that there must be a net

attractive interaction if islands are to form, even though there may be a

short-range repulsion.

Phase transitions for such lattice gas/solid systems must also occur at low coverages, but have so far been little investigated.[14a] They are of interest here because they may represent a fundamentally different phenomenon than saturation-coverage transitions and as such can give added quantitative information on adatom interactions. This can be illustrated in the following way. Assume an overlayer system with ordered structure different from (1x1), e.g. p(2x1), c(2x2) etc., requiring vacant sites on the surface even at the saturation coverage for that particular structure. This implies short-range repulsions that prevent close packing of adatoms. In terms of a quasichemical model, one can think of this over-layer as an ordered two-dimensional binary alloy A_xB_{1-x}, of definite stoichiometry (more precisely a compound) where A refers to adatoms and B to vacancies, with a free-energy preference for AB pairs relative to AA or BB pairs in the ordered state. Specifically for an ordered layer corresponding to half coverage at saturation, there are an equal number of adatoms and vacancies on the surface and $x = 1/2$.

At much lower than saturation coverages, this adsorbate may produce islands of the same ordered structure, but these exist in a much larger region of empty substrate, or "sea". Equivalently one can think of a two-phase region with precipitates of the compound A_xB_{1-x} (phase 1) in the "sea" (phase 2). As the temperature rises, these islands may prefer to "dissolve", with atoms leaving the ordered regions distributing them-selves randomly on sites in the "sea". To do this, only the attractive

interaction leading to the existence of ordered regions needs to be overcome. An equivalent description would be in terms of a two-dimensional evaporation from the island, the analog to three-dimensional sublimation or dissolution of solute in solvent. Conversely, one could speak of a two-dimensional condensation as the temperature is lowered.

On the other hand, at saturation coverage for a particular ordered structure, only the A_xB_{1-x} phase and no "sea" exists. Hence the above mode of disordering as the temperature rises is no longer possible. Now a true order-disorder transition takes place, with atoms randomly moving from their ordered-lattice sites to other, more repulsive, sites on the surface. Again using the analogy of a two-dimensional binary alloy of stoichiometry corresponding to the fractional coverage of adsorbate (A_xB_{1-x}), this phase transition removes the preference for AB pairs and at high enough temperatures makes the distribution of adatoms and vacancies as random as the stoichiometry will allow. For half coverage, this is completely random. The lower the energy of the AB pairs relative to the average of the AA and BB pairs, the higher will be the disordering temperature for the ordered structure.

Hence in adsorbate systems with net attractive adatom interactions, the observed phase transitions should be interpretable in two limits, a dissolution (conversely condensation) transition at low coverage and an order-disorder transition at saturation coverage for a given structure. The former is a measure of the net attractive interaction, while the latter involves overcoming the repulsive short-range interaction. Since this short range repulsion prevents the formation of a (1x1) pattern, it must

be greater than the net attractive interaction leading to island formation. Hence the transition temperature for the saturation coverage order-disorder transition is expected to be higher than that for the low-coverage transition.

In this paper, we report measurements of LEED superlattice beam intensities and angular profiles for W(110)p(2x1)-O for a wide range of coverages. O on W(110) forms a "closed" system in that it is not in equilibrium with either the bulk or the gas phase, i.e., the coverage stays constant as a function of temperature over the temperature range of interest here. Hence the measurements should be interpretable in terms of thermodynamics of two-dimensional systems. The p(2x1)-O structure, shown in Fig. 1, consisting of doubly spaced rows parallel to <111> directions and corresponding at saturation to half-monolayer coverage, requires a short-range repulsion in addition to the net attraction required to form islands. We observe phase transitions at two limiting transition temperatures over the range of coverages over which we are able to observe diffraction, $\simeq$ 460°K at low coverage and $\simeq$ 720°K at saturation coverage. We interpret these, as discussed above, in terms of two-dimensional dissolution of islands and an order-disorder transition respectively.

In the next section we discuss experimental details and in Section III the analysis of the measurements. In Section IV we compare the high- and low-coverage transitions and discuss these in terms of a partial phase diagram for this chemisorbed layer. A theoretical explanation for these phase transitions and a fit to the data to extract adatom interaction energies will be given in a separate paper.

II. EXPERIMENTAL

Some details of the apparatus used in this work have been discussed previously.[17] It is a simple LEED diffractometer with two-circle-gonio-

meter, moveable Faraday cup collector and small fluorescent screen, pumped by an orbitron electrostatic getter-ion pump with pumping speed for active gases 150 l/sec, limited by tube conductance. Typical base pressures are in the low 10^{-10} torr range, with partial pressures of CO, CO_2, and H_2, measured by a residual gas analyzer, in the 10^{-11} torr range or lower. The Faraday collector consists of a grounded plate with variable aperture and a deep cup several times the diameter of the defining aperture. The cup itself is biased to accept electrons within 1eV of the incident beam energy. This arrangement[18] because it does not require intermediate grids, permits precise measurement of the angular distribution J vs. ϑ of the diffracted intensity without the distorting influence of retarding grids.[19] In the measurements reported here a 1mm diameter aperture was used. The cup was both guarded and shielded, but at the highest crystal temperatures used in the experiments (900°K), the leakage current across the insulators in the cup became $\sim 10^{-13}$A, of the same order of magnitude as some of the measured signals. This leakage was reduced by an order of magnitude by cooling the detector to as low as 180°K by connecting it via a flexible Cu braid to a LN_2 cold finger.

The W(110) sample was polished and oriented to within 1/2° of [110] and cleaned in UHV in the usual manner.[20] The sample was mounted on two W rods that were clamped in a massive Cu block, and heated from underneath with a W filament. Both radiation heating and electron bombardment were possible, with the Cu block acting as a radiation shield and heat sink to keep the surrounding goniometer cool. Electron bombardment at 1kV and 50mA heated the sample to 2500°K in several seconds. Radiation

heating to 1000°K was possible. To eliminate magnetic field effects on the diffraction due to current in the heater filament, the filament was operated with half-wave rectified current, with the diffracted intensity measured in the off half cycles. Temperatures were measured with a ~.01mm W 3%Re-W25%Re thermocouple spotwelded to the edge of the crystal.

After the sample was clean, contamination buildup over time was mostly CO and H. The presence of H (as well as CO) could be detected quite sensitively by observing the diffuse intensity near the Brillouin zone boundary in scans of I vs. ϑ. Flashing to 600°K several times removed all hydrogen (as evidenced by the absence of a desorption peak in the mass spectrometer) and resulted in reduction of the diffuse intensity. Alternately, a flash to 2300°K to remove all ambient contaminants produced sharp angular profiles with intensity minima in I vs. ϑ at the zone boundaries that were near noise levels.

The response function of the system, discussed in detail elsewhere[21] was determined by measuring the angular distribution of intensity J vs. ϑ for diffracted beams as a function of diffraction conditions for a surface prepared in the above manner. Figure 2 shows such a profile for the (00) beam from the clean surface. Approximating this shape as Gaussian[22] the full width at half maximum of its Fourier transform , called the transfer width,[23] is a measure of the coherence length of the instrument. It has a value between 40 Å and 140 Å, depending on diffraction geometry and energy of the incident beam, similar to values determined for other Faraday cup systems.[23] For any incident angle and

energy, different beams, of course, have different angular widths and transfer widths. The angular widths at the position of the superlattice beams are inferred by interpolation between the two nearest clean-surface beams.

Incident-beam currents used in these studies were $\sim 10^{-7}$A, with reflected maximum beam intensities typically $\sim 10^{-10}$A for the fundamental and 10^{-11}A for the superlattice reflections. At higher temperatures, the superlattice reflections decrease into the 10^{-12} to 10^{-13}A range.

Oxygen exposures were made through a beam tube using a Ag permeation leak as source, typically using pulses of maximum pressure $P = 1 \times 10^{-9}$ torr and duration about 1/2 min. to 1 min. Sticking coefficient measurements of Gomer et al[24] were used to convert exposures to coverages, using as normalization $\theta = 0.5$ for the "best" p(2x1) pattern, as determined by the maximum in $J_{superlattice}$ vs. exposure curves. Although this is a frequently used procedure for determining sticking coefficients[25] or to convert exposures to coverages, it appears not to have been recognized that the shape of $J_{superlattice}$ vs. coverage (and hence the determination of J_{max}) depends on the coherence width of the instrument as well as interference effects, with exposures for $J_{supperlattice}^{max}$ varying in our particular case by $\pm 15\%$, depending on the energy of the incident beam or the diffraction conditions of the measurement. This is discussed in greater detail later; here this uncertainty is indicated by error bars in the figures involving coverage.

Measurements include the angular distribution of intensity as a function of coverage and temperature for both substrate and superlattice beams.

Angular distribution measurements for the clean surface give the instrument response and details of the thermal diffuse scattering background. The angular distribution of intensity in superlattice beams gives a measure of the average island size, and as a function of temperature allows determination of the transition temperature.

III. ANALYSIS OF MEASUREMENTS

A. Temperature Dependence of the Peak Intensities for the p(2x1)-O Structure.

The saturation coverage W(110)p(2x1)-O structure has been the subject of considerable discussion,[26] with several studies dealing with the order-disorder transition.[10,14,25] In measurements of the intensity of a superlattice reflection as a function of temperature, it is observed that the intensity at first decays exponentially and at higher temperatures more rapidly than exponentially, as shown in Fig. 3. The exponential region is interpreted in terms of an effective Debye-Waller factor, while the more rapid decay indicates some sort of order-disorder transformation.

1. Debye-Waller Factor

Measurements of the intensity decay of beams diffracted from the clean surface give a measure of the effective Debye-Waller factor of W(110) surface atoms, and thus of the effective mean square vibrational amplitude of these atoms along the diffraction vector (nearly normal to the surface). As expected from similar studies[27] the slope of ln J vs. T is steeper than measurements with x-ray diffraction from the bulk, indicating a larger surface mean square vibrational amplitude. Using a model[18] taking into account the penetration of the electron

beam as well as the decay of excess vibrational amplitude away from the surface gives a value of 2.5 ± 0.5 for the ratio of mean square vibrational amplitude for the outer layer of W(110) atoms to bulk W atoms.[28] Theoretical studies[29] arrive at somewhat smaller values.

After adsorption of oxygen similar ln Jvs. T measurements on superlattice beams always give the same slope as for the clean surface far below the phase transition. This slope measures the effective mean square vibrational amplitude of the overlayer/substrate system normal to the surface. Since at these temperatures the O/W mass dependence of the vibrational amplitude becomes negligible,[30] the implication is that the vibration of O against W is much less than the vibration of the outer W layer. Thus the O essentially "rides along" with the W. Further, since the vibrational amplitude is a measure of the force constant and hence the curvature of the potential well near its minimum, it is clear that the shape of the O/W potential well in the z direction is much steeper than the W-W surface potential well. This may not be surprising in view of the large binding energy (~6 eV) of O on W(110).[31] Although no direct correlation between binding energy and force constant need exist, in other, more weakly bound systems the overlayer force constant is also less and the slope of the Debye-Waller factor correspondingly steeper.[11] Unfortunately, nothing more quantitative can be said about the O/W force constant without low-temperature measurements, where the mass dependence of the vibrational amplitude would help to separate the substrate and adsorbate vibrations.

2. Evidence of Phase Transition

Figure 3 shows that above a certain temperature, the intensity of the superlattice beams decays more rapidly than expected from a disordering due only to thermal vibrations. Hence, some further displacement disorder with atoms actually leaving equilibrium sites must be occurring. In an earlier paper[10] we have shown that this disordering is substitutional, i.e., that there is a place exchange between adatoms and vacancies, but that the type of site on the surface is the same. This corresponds to a classic substitutional order-disorder transition.

However, it was also observed that the angular width of the diffracted beam increases with temperature in the range of the transition, indicating a lack of long-range order, and an effective decrease in average size of coherently scattering domains with increasing T. Since this can affect both the shape of the intensity decay and the determination of the transition temperature, the angular width of the diffracted beams and the effect of the instrument on the measurement were investigated in more detail.

B. Angular Width of Superlattice Beams.

In Fig. 2 an angular profile of a substrate beam was shown. In the limit assumed here, that the clean surface is rigid, infinite, and laterally perfectly periodic,[32] it provides a diffracted beam with a delta-function angular distribution, and the measured angular width is all due to instrumental parameters such as detector aperture, beam divergence, and source extension.

Modeling of the instrument function using reasonable values for these parameters leads to angular widths very close to those measured.[21]

Any measurement of a diffracted beam from the surface under different conditions, e.g. with an adsorbed layer, then can be represented as the convolution of the actual diffracted signal $I(\underline{S}_{||})$ and the instrument response $T(\underline{S}_{||})$ for a given $\underline{S}_{||}$, the parallel component of the diffraction vector,

$$J(\underline{S}_{||}) = I(\underline{S}_{||}) * T(\underline{S}_{||}). \tag{1}$$

It is evident from convolutions involving a delta function that in the limit of a diffracted beam that is very narrow (small angular width) the shape of the measured signal is that of the instrument function, whereas for a very broad signal, the angular width due to the instrument has little effect and the measured angular shape is very similar to the actual diffracted beam shape.

In adsorbate systems, the average size of the perfectly ordered regions on the surface is reflected in the angular shape I vs. ϑ of the superlattice diffracted beams. If at any given coverage the temperature is low enough so that islands do form, thermodynamic equilbrium requires that only one (very large) island exist, and hence that the diffracted beams be as sharp as the instrument function. However, frequently some angular broadening is observed,[1,25] and is interpreted in terms of average island sizes smaller than the coherence width of the instrument.

An example of the angular width of the (1/2 1/2) superlattice beam as a function of coverage is shown in Fig. 4, for O adsorbed at room temperature and annealed at ~425°K for extended times until the minimum angular widths were obtained. It is seen that at low coverages the full width at half maximum of the angular distribution is several times as wide as the instrumental response width, which represents the narrowest angular width observable. As the coverage increases, the measured superlattice angular width approaches the instrumental width, indicating that the actual diffracted signal is becoming sharper, i.e., the domains of ordered structure are getting larger. Of course, different angular widths at a given coverage are measured at different energies, as expected from simple diffraction theory, and different limits are approached at high coverage because of the dependence of the instrument response on energy.

It is interesting to note that the measured angular widths are so broad. One would expect that for a perfect substrate and sufficient annealing, that island growth analogous to recrystallization in the bulk would take place. This is not the case;[21,25] even at the lowest measured coverages, there are many more adsorbed atoms than are necessary to make ordered regions many times the size of the instrument coherence and thus diffracted beams as sharp as the instrument function. We nevertheless/may expect that the measured distribution of islands represents an equilibrium state,[21] but for an imperfect substrate surface that exhibits heterogeneity, so that the actual surface consists of many smaller (perfect) surface regions with effectively infinite walls between them, e.g. due to steps. Such clean-surface

heterogeneity manifests itself in modulation of the angular width of the substrate beams.[33] This has been observed for W(110) and will be presented elsewhere.[34] The effect of small island size on thermodynamic quantities is to depress disordering temperatures. This is discussed in more detail below.

A quantitative determination of the actual signal intensity and line shape $I(\underline{S}_{||})$ is possible by deconvoluting the measured signal $J(\underline{S}_{||})$ with the instrument function. This is a useful procedure as long as the signal is broad but unfortunately leads to large uncertainties when the signal is narrow compared to the instrument/ response. However, since the line shapes are nearly Gaussian (Fig. 2), an adequate determination of the width of $I(\underline{S}_{||})$ is obtained by assuming that both $I(\underline{S}_{||})$ and $T(\underline{S}_{||})$ are Gaussians. Very simply it can be shown that

$$b_I = (b_J^2 - b_T^2)^{1/2}, \qquad (2)$$

where b_J, b_I, b_T represent the FWHM of the Gaussians. These angular widths in reciprocal space can now be interpreted in terms of a coherence width in real space, (i.e., island size distributions) assuming some model. Although we will use results of such island size determinations in estimating size effects, the details of this procedure are not germane to the present discussion, and will be treated separately.[21] Here only the intensity $I(\underline{S}_{||})$ is of interest.

C.   Intensities of Superlattice Beams.

From Eq. 1 it is clear that the measured intensities are also affected by the instrument response. This has already been alluded to in Sec. II in discussing the determination of saturation coverage from maximum

intensities in $J_{superlattice}$ vs. θ. Again assuming that line shapes are Gaussian, it is easy to show that

$$J(\underline{S}_{||}) = \frac{b_I \ I(\underline{S}_{||})}{(b_T^2 + b_I^2)^{1/2}} , \qquad (3)$$

where b_I and b_T respectively are the FWHM of the Gaussian profiles of the signal and the instrument function. Two limits are recognizable. When the instrument function is quite narrow relative to the signal (e.g. at low coverages), $J(\underline{S}_{||}) = I(\underline{S}_{||})$ and a measurement of the peak intensity faithfully reproduces the actual signal intensity. In the other limit that the instrument function is very wide

$$J(\underline{S}_{||}) = \frac{b_I I(\underline{S}_{||})}{b_T} , \qquad (4)$$

and the measured intensity is some constant fraction of the actual signal as long as both b_T and b_I are constant.

Again, two cases occur. First b_T may change, and does if the intensity, for example, is measured at different energies or diffraction conditions. It is this that makes the determination of the saturation coverage for a given structure uncertain. If this measurement is taken at different energies, thus making b_T different, the maximum in $J(\underline{S}_{||})$ will occur at different θ as long as $b_T \gtrsim b_I$. More important for the present work, however, is the interpretation of $J(\underline{S}_{||})$ vs. temperature in terms of $I(\underline{S}_{||})$ vs. temperature. Since these measurements are made at constant b_T, the only dependence is on b_I. If b_I does not change then J and I are simply related by a constant. An example of this is the measurement of Deybe-Waller factors from clean surfaces, where the angular profile

stays the same with temperature, and hence the slope is not affected.

If b_I changes, as we have already indicated it does for thermal disordering of the 0 overlayer on W(110), the decay of the actual signal intensity $I(\underline{S}_{||})$ is different from that of the measured $J(\underline{S}_{||})$, and the measurements must be corrected with Eq. 4. Figures 5 and 6 show respectively the intensity *decay of the (1/2 1/2) beam* with temperature for high and low coverage along with the instrument-corrected curves. It should be noted that since the diffraction geometry here was chosen so that $b_I > b_T$, the correction is not significant for low coverage at any temperature. This need not be the case, if, for example, a much worse instrument or a low enough energy is chosen, so that $b_T \gtrsim b_I$. For example, fluorescent screen systems may not be able to observe such transitions. At high temperature for high coverage, since again the diffracted beams are broad, the correction is small. Only at low temperatures and high coverages is there a large difference in the curves, leading to some differences in the actual shape of the intensity decay. All curves used in the next section have been corrected for instrument function, and are labeled $I^{max}_{superlattice}(T)$.

IV. PHASE TRANSITION AS A FUNCTION OF COVERAGE.

The $I^{max}_{superlattice}$ vs. T measurements discussed in the last section were repeated at a number of different coverages for the p(2x1)0 structure, up to saturation coverage. For each particular coverage, angular widths I vs. ϑ were measured. Examples of the data for the (1/2 1/2) beam at both high and low coverage were shown in Figs. 5 and 6.

To extract the intensity decay due to the phase transition requires
the removal of the intensity decay due to the Debye-Waller factor, given by
the linear part of the curve, e.g. in Figs. 5 and 6. As already indicated,
for saturation coverage this slope is the same within experimental
uncertainty as the slope for clean W(110). At low coverage, since the
transition begins much earlier, and since experiments with sample temperatures
below room temperature were not possible, little linear region is evident.
However, since the ordered structure is the same independent of coverage,
and since the Debye-Waller factor in these experiments measures vibrations
nearly normal to the surface, for which contributions of lateral interactions
would in any case be small, the use of the same linear slope is justified
independent of coverage.

The actual decay of intensity due to disordering of the overlayer islands
at high and low coverages is finally shown in Fig. 7. It is clear from
these curves that not only is the transition temperature as defined by the
inflection point in the curves different, but that the shape of the curve is
different, with the low coverage intensity reaching a constant value at
high temperatures. At intermediate coverages, the intensity decay is
more complicated. As the coverage is increased the intensity decay appears to
consist of two or more transitions, as illustrated in Fig. 8. The low-
coverage transition becomes weaker but appears to have an inflection point at
or near the same temperature, while a coverage dependent higher-temperature
transition grows stronger, until at saturation for the p(2x1) structure
only the highest-temperature transition is observed. It is difficult to
assign a transition temperature to this complicated decay; in Fig. 9

are shown only the low-coverage and high-coverage transitions (defined as inflection points) as long as these are reasonably distinct. However, it should be kept in mind that the intermediate coverage behavior is more complicated than indicated by this figure.

V. DISCUSSION

There are two approaches to explaining the observed phase transition behavior with coverage. We choose first the simpler in assuming a limited interaction range for atoms of a lattice solid consisting of oxygen atoms and vacancies. This compound of p(2x1) structure has a very highly negative free energy of formation, i.e. it precipitates out of a very dilute solution of O atoms on the surface if the mobility of the O atom is sufficiently great. Thus even at very low coverages p(2x1) islands are formed. These now may undergo a transition to the two-dimensional vapor or lattice gas at sufficiently high temperatures. As observed in Monte Carlo calculations,[35] a nearly constant transition temperature is obtained over a wide range of coverages if the interaction energy is large. As this interaction is reduced, the transition temperature is expected to fall more rapidly as the coverage is lowered.

At the saturation coverage, the low-temperature state is a single phase of definite stoichiometry, the p(2x1) oxygen-vacancy compound. It undergoes a phase transition to a substitutionally disordered single phase consisting of an equal number of O atoms and vacancies with random occupation of sites. The transition temperature is related to the difference between the net attractive and repulsive adatom interaction energies

Based on this picture, a partial phase diagram can be constructed for the disordering of the p(2x1)-O overlayer as shown in Fig. 10a. At sufficiently low temperature, the system can be thought of as a two-phase mixture consisting of p(1x1) "sea" and p(2x1) island "precipitates". At very low coverages and high temperature, the O overlayer exists as a lattice gas that gets increasingly dense as the coverage increases. The system at high temperature can also be thought of as a single disordered-alloy phase of p(1x1) structure, with O atoms randomly distributed throughout it. At the saturation p(2x1) coverage the transition corresponds to a congruent point.

In this interpretation, all transitions are assumed to be first-order. However, calculations show[35] that over part of the coverage and temperature range transitions can be second-order. This requires the p(2x1) phase to have a much wider coverage range of stability, i.e., the p(2x1) phase should be stable even with a very large concentration of vacancies in it. Thus an alternative phase diagram, as shown in Fig. 10b, would restrict the two-phase region and broaden the p(2x1) phase region.

In the ideal case, it should be possible to distinguish these two models using low-energy electron diffraction. A second-order transition such as at $\theta = 0.4$ in Fig. 10b requires that the p(2x1) phase form uniformly (and immediately) over the whole surface. This means that the overlayer will have long-range order and the superlattice diffraction beams will be as sharp as the instrument allows. On the other hand, a first-order transition such as at $\theta = 0.2$ in Figs. 10a or 10b from a one-phase to a two-phase region requires the precipitation of small islands and thus the superlattice diffraction features should initially be quite broad and only become narrow as these islands grow. Similarly a transition at $\theta = 0.4$ at lower

temperature, from the p(2x1) phase to a two-phase region, will be first-order and accompanied by the precipitation of islands of "denser" p(2x1) phase, and the diffraction features ought to broaden as this phase boundary is crossed.

In practice, this differentiation is much harder to make than indicated, for three reasons. One, the instrument in any case limits the coherent regions that one can observe to something of the order of 200Å. Second, substrate surface heterogeneity may limit the order to distances smaller than this. Third, even without the substrate heterogeneity, antiphase domains form on this surface, and if there is little driving force for the formation of only one domain, smaller coherent regions are present. Four antiphase domains are possible, two translational ones for each of two orientations. The domains of different orientation do not interfere, and as such one acts as an extended defect for scattering from the other. Experimentally on well-prepared (110) surfaces the diffraction features from these domains are equally bright.

In spite of these difficulties, the evidence indicates that at low coverage the transition is from a one-phase to a two-phase region and hence first-order. Diffraction spots are quite broad at high temperatures and there is a continuous beam narrowing as the temperature is lowered. This is inconsistent with a second-order transition, which would require the diffraction features very quickly to be as sharp as allowed by sub- strate heterogeneity or the instrument. At or below $\theta = 0.25$, a stable, single p(2x1) phase (containing now 50% more vacancies than the "dense" p(2x1) phase at $\theta = 0.5$) is in any case doubtful, since on the average this would require small p(2x2) regions to appear. These have never been observed.

At higher coverages, the identification is less clear. Again, if the transition is second-order, the diffraction features should become sharp rapidly as the phase boundary is crossed. However, even if the transition

is first-order, one may expect a much more rapid narrowing in diffraction features than at low coverages, because at the higher temperatures involved, coarsening should be more rapid. In the absence of surface heterogeneity, the instrument will limit the size of island observable; this limiting size may very rapidly be achieved for the first-order transition and thus no differentiation as to the order of the transition could be made. In fact, the experiment indicates that surface heterogeneity may limit the size of substrate coherent regions to the order of or slightly smaller than the instrument coherence. This provides the possibility of distinguishing the order of the transition, since for this case the substrate consists of many small, independent surfaces, and the argument is the same as for the ideal case, without regard to instrument function. However, experiments in this intermediate coverage range are at present not accurate enough to do this.

The second view would consider the p(2x1) structure as two-dimensional solid O. Such a model appears to be more appropriate for the close-packed physisorbed structures such as Kr on graphite[16] than for a non (1x1) lattice solid where only every other equivalent site is occupied. The more appropriate analog would be the full-monolayer p(1x1)-O layer on W, although even this is not precisely the same. The difficulty with the p(2x1) structure is in interpreting the saturation coverage order-disorder transition in terms of a melting phenomenon, since in the high-temperature phase the same sites are occupied, only in a random fashion, whereas a liquid has a much different pair distribution function. In the first picture, the disordered phase is considered as a disordered solud solution. Here it might be considered a lattice liquid, or a lattice gas, depending on the range of adatom interactions. Since it is known that these extend to more than nearest neighbors for this overlayer it is clear that "lattice gas" is not a proper description for the disordered state at saturation. In fact, this must be

true already at lower coverages. If for a lattice gas it is assumed that the occupied sites are statistical and noninteracting, they must be far enough separated to be outside the range of A-A interactions. Using the minimum range of interactions necessary to explain the p(2x1) structure, as shown in Fig. 1, and letting all larger-range interactions equal zero, the maximum density of noninteracting atoms in the sea can be only 0.25, i.e., an ideal lattice gas should be possible in this system only below $\theta = 0.25$, and perhaps even lower if longer - range interactions are present. This also implies that complete island dissolution (sublimation) to a lattice gas is not possible above $\theta = 0.25$, independent of which picture is adopted for the solid phase.

Assuming that one can describe the p(2x1) structure as solid 2-D oxygen, by analogy with phase diagrams for three-dimensional, single-component solids, the transition temperature vs. coverage should follow the same behavior as the phase boundary in T-V diagrams. A constant T_t with coverage would then imply melting along the triple-point line,[36] with solid, liquid, and vapor all in equilibrium. This would occur at intermediate coverages; at low coverages the dependence of T_t on θ is related to the vapor pressure, but may in fact be very slight if the vapor pressure is quite low. The observed nearly constant T_t would then be this triple-point melting line. A possible phase diagram for this model is shown in Fig. 10c.

The relationship of these two views of the observed phenomenon depends on what is meant by lattice liquid and how it corresponds to a true liquid. This is at the moment unclear. As regards the very low coverages, these two

views are consistent if one assumes in the latter that the observed low-coverage T_t is the upper limit to the solid-vapor phase boundary. This is equivalent to saying that at the lowest observed coverage and below, a solid-vapor transition is effective. That we have actually reached the coverage where this is true is not certain; however, the magnitudes of the interactions derived from a dissolution model are not affected, since this model is independent of coverage as long as it is low if the vapor pressure dependence on coverage is taken into account. As indicated earlier, this dependence may be quite weak, so that in fact T_t for the solid-vapor transition may also appear essentially flat.

Construction of a phase diagram in general implies equilibrium for "macroscopic" systems. However, if particles become quite small, the surface makes a contribution to thermodynamic functions, with a resultant depression of transition temperatues. These effects become noticeable for nucleus diameters of $\approx 200\overset{\circ}{A}$, and become significant for much smaller diameters. A similar effect should occur for islands. Because these islands are quite small, $\approx 35\overset{\circ}{A}$,[21] island boundary effects may be significant, with transition temperature as much as 30% less than would be observed for macroscopic islands. Since the average size of the islands increases with coverage, another possibility for the changing transition temperature with coverage is its size dependence. However, since the average size of islands changes by less than a factor of two, the observed change in T_t would appear to be too large. Furthermore, a smooth change with T_t is expected, since the size changes uniformly. Finally, at any given coverage a sharpening of the super-lattice reflections as a function of temperature should result as the

smaller islands disorder. This is not observed; whether it is observable depends of course on the distribution of island sizes.

It is thus improbable that the dependence of T_t on coverage is simply a size effect. In any case, the phase boundaries should be interpreted in terms of lower limits to macroscopic-island thermodynamic functions.

VI. CONCLUSION

In this paper we have described experimental results for the thermal disordering of an island-forming chemisorbed overlayer, W(110) p(2x1)-0, as a function of coverage. The results can be interpreted in the low-coverage limit as the dissolution of islands and at saturation coverage as an order-disorder transition for the p(2x1) structure. The fact that distinct adatom-adatom interactions are important in these phase transition allows their separate determination. This is the subject of a later paper,[21] in which we give a theoretical interpretation of the phase transitions shown here and determine from a model fit to the data adatom-adatom interaction energies in this system. Additional information about these interactions can be obtained from a study of the 0/W(110) system at coverages above $\theta = 0.5$, where a new ordered structure [p(2x2)] forms. Preliminary data for the (1/2 1/2) beam were shown in Fig. 9; however, to gain new information, the same measurements must be performed on beams such as the (10) beam, which arise due to the p(2x2) structure. Such studies are presently underway.

ACKNOWLEDGEMENTS

REFERENCES

1. See, for example, a) J. May., Adv. Catal. 21, 151 (1970);
   b) G. A. Somorjai and H. H. Farrell, Adv. Chem. Phys. 20, 215 (1972).

2. L. W. Bruch, P. I. Cohen, and M. B. Webb, Surface Science 59, 1 (1976).

3. T. L. Einstein and J. R. Schrieffer, Phys. Rev. B7, 3629 (1973);

   J. Koutecky, Trans. Faraday Soc. 54, 1038 (1958);

   T. B. Grimley and S. M. Walker, Surface Sci. 14, 395 (1969) and references there;

   J. R. Schrieffer in Collective Properties of Physical Systems, eds. S. and B. Lundqvist, Academic (1973) and references there.

4. See, e.g., G. Ertl and J. Koch in Adsorption-Desorption Phenomena, ed. F. Ricca, Academic Press (1972), pg. 345.

5. For a review, see D. A. King, CRC Reviews of Solid State Sciences (1978, to be published). See also D. L. Adams, Surface Sci. 42, 12 (1974), D. A. King, Surface Sci. 47, 384 (1975).

6. For a review, see T. T. Tsong, CRC Reviews of Solid State Sciences (1978, to be published); G. Ayrault and G. Ehrlich, J. Chem. Phys. 60, 281 (1974), T. T. Tsong, Phys. Rev. Letters 31, 1207 (1973).

7. a) A. U. MacRae, Surface Sci. 1, 319 (1964);

   b) J. J. Lander, Surface Sci. 1, 125 (1964);

   c) J. J. Lander and J. Morrison, Surface Sci. 6, 1 (1967).

8. a) P. J. Estrup, Physics Today 28, No. 4, 33 (1975);

   b) P. J. Estrup in The Structure and Chemistry of Solid Surfaces, ed. G. A. Somorjai, Wiley, New York (1969).

9. a) J. C. Tracy and J. M. Blakely, Surface Sci. 15, 257 (1969); in The Structure and Chemistry of Solid Surfaces, ed. G. A. Somorjai, Wiley, New York (1969).

   b) J. C. Tracy, J. Chem. Phys. 56, 2736 (1972).

10. J. C. Buchholz, Ph.D. dissertation, Univ. of Wisconsin-Madison (1974)

    J. C. Buchholz, and M.G. Lagally, Phys. Rev. Letters 35, 442 (1975).

11. P. I. Cohen, J. Urguris, and M. B. Webb, Surface Sci. 58, 429 (1976).

12. M. D. Chinn and S. C. Fain, Phys. Rev. Letters 39, 146 (1977).

13. G. Doyen, G. Ertl, and M. Plancher, J. Chem. Phys. 62, 2957 (1975).

14. G. Ertl and D. Schillinger, J. Chem. Phys. 66, 2569 (1977).

14a. Recent extensive measurements have been performed for H/Mo(100),
    C.H. Huang and P.J. Estrup, to be published.

15. See, for example, G. Ertl and J. Küppers, Surface Sci. 21, 61 (1970);
    G. Ertl and M. Plancher, Surface Sci. 48, 364 (1975); Ref.14.

16. Heat capacity measurements as a function of coverage for physisorbed
    layers have shown evidence for a coverage-dependent transition
    temperature. T.-T. Chung and J. G. Dash, J. Chem. Phys. 64, 1855
    (1976), J. G. Dash, private communication.

17. J. C. Buchholz, G.-C. Wang, and M. G. Lagally, Surface Sci. 49, 568
    (1975).

18. E. R. Jones, Jr., J. T. McKinney, and M. B. Webb, Phys. Rev. 151,
    476 (1966).

19. M. B. Webb and M. G. Lagally, Solid State Physics 28, 301 (1973).

20. P. A. Jacquet, Met. Rev. 1, 157 (1956); J. A. Becker, E. J. Becker, and
    R. G. Brandes, J. Appl. Phys. 32, 32 (1961).

21. G.-C. Wang, T.-M. Lu, and M. G. Lagally, to be published.

22. The actual shape is Gaussian in the peak, with wings more nearly
    Lorentzian.

23. R. L. Park, J. E. Houston, and D. G. Schreiner, Rev. Sci. Instrum.
    42, 60 (1971).

24. C. Wang and R. Gomer, Proc. 7th Intern. Vac. Congr. and 3rd Intern.
    Conf. Solid Surfaces (Vienna 1977) (to be published).

25. See, for example, T. Engel, H. Niehus, and E. Bauer, Surface Sci.
    52, 237 (1975).

26. See ref. 1a, pg. 225 and references there; Ref. 9a; Ref. 10; Ref. 17.
    A recent summary is given in Ref. 25.

27. Ref. 18; W. N. Unertl and M. B. Webb, Surface Sci., 59, 373 (1976).

28. M. G. Lagally, J. C. Buchholz, and G.-C. Wang, Bull. Am. Phys. Soc. 20, 490 (1975).

29. C. Cheng and R. Wallis, Bull. Am. Phys. Soc. 20, 489 (1975).

30. R. E. Allen, G. P. Alldredge, and F. W. deWette, J. Chem. Phys. 54, 2605 (1971).

31. C. Kohrt and R. Gomer, J. Chem. Phys. 52, 3283 (1970).

32. This is the usual assumption for clean surfaces. However, surface steps may exist, leading to physical broadening that varies with energy. See Ref. 33.

33. For an excellent review of such effects, see M. Henzler in Electron Spectroscopy for Surface Analysis ed. H. Ibach, Springer (Berlin) (1977).

34. G.-C. Wang and M. G. Lagally, in preparation.

35. K. Binder and D. P. Landau, Surface Sci. 61, 577 (1976).

36. J. G. Dash, private communication.

Fig. 1   Schematic diagram of a p(2x1) island on a bcc (110) sub-
           strate, corresponding to the W(110)p(2x1)-O structure.
           filled circles: substrate atom equilibrium positions;
           crosses: overlayer atoms. The lateral placement of over-
           layer atoms is arbitrary. Crosses at random sites indicate
           the overlayer solubility of atoms in the "sea" at any
           finite temperature and coverage.

Fig. 2   Angular profile J vs ϑ for the clean-W(110) (00) beam at
           an incident-electron energy E = 87eV, angle of incidence
           ϑ_0 = 7°, and azimuthal angle ϕ = 64.75°. Solid circles
           are a Gaussian fit to the line shape.

Fig. 3   Temperature dependence of LEED reflections: curve a, super-
           lattice reflection showing order-disorder transition, (1/2 1/2)
           beam, 24 eV, $_0$= 6°; curve b, clean substrate, (00) beam,
           54 eV, $_0$= 6°; curve c, O-covered substrate, (00) beam, 132 eV,
           $_0$ = 7°.

Fig. 4   Measured angular width $\Delta\vartheta_{1/2}$ of the (1/2, 1/2) super-
           lattice reflection as a function of coverage for a
           well-annealed oxygen-overlayer. θ = 0.5 corresponds to
           saturation coverage for the p(2x1) structure. The dotted
           line indicates the instrumental width at the conditions
           of the measurement, E = 52eV, ϑ_0 = 0°, ϕ = 35.25°.

Fig. 5   Temperature dependence of the intensity and angular width
           a $\Delta\vartheta_{1/2}$ of the (1/2,1/2) superlattice reflection at high
           coverage, θ = 0.5. O: measured peak intensity; X: signal
           intensity after instrument response correction. Dashed
           line represents smooth curve through measured angular
           widths; dotted line indicates instrument width at the
           diffraction conditions of the measurement, E = 79eV,
           ϑ_0 = 0°, ϕ = 35.25°.

Fig. 6   Temperature dependence of the intensity and angular width
           of the (1/2, 1/2) superlattice reflection at low coverage,
           θ = 0.14. O: measured peak intensity; X: signal intensity
           after instrument response correction. Dashed line represents
           smooth curve through measured angular widths, dotted line
           indicates instrument width at the diffraction conditions of
           the measurement, E = 80eV, ϑ_0 = 0°, ϕ = 35.25°.

Fig. 7   Decay of the normalized intensity of the (1/2, 1/2) beam
           with temperature at high and low coverages. ▲ θ = 0.14, ●:
           θ = 0.5. E = 80eV, ϑ_0 = 0°, ϕ = 35.25.

Fig. 8   Decay of the normalized intensity of the (1/2, 1/2) beam
           with temperature at an intermediate coverage, showing the
           low-temperature transition followed by more complex behavior
           at higher temperatures. $\theta = 0.2$.

Fig. 9   Transition temperature for disordering of the p(2x1)-O
          overlayer vs coverage. $\theta = 0.5$ corresponds to saturation
          coverage for the p(2x1) structure. The inflection point
          in the intensity decay of the (1/2 1/2) beam with tempera-
          ture at various energies is plotted, where this point is
          reasonably clear.

Fig. 10   Possible phase diagrams for W(110)p(2x1)-O.
          a) Considering the p(2x1) structure as a compound with
          narrow range of stability and assuming first-order transi-
          tions only.
          b) Considering the p(2x1) structure to exist over a broader
          range of coverage and allowing second-order transitions.
          c) Considering the p(2x1) structure as solid two-dimensional
          oxygen and taking the T-V cut through the phase diagram of
          a monocomponent system.

[1̄11]

[1̄11]
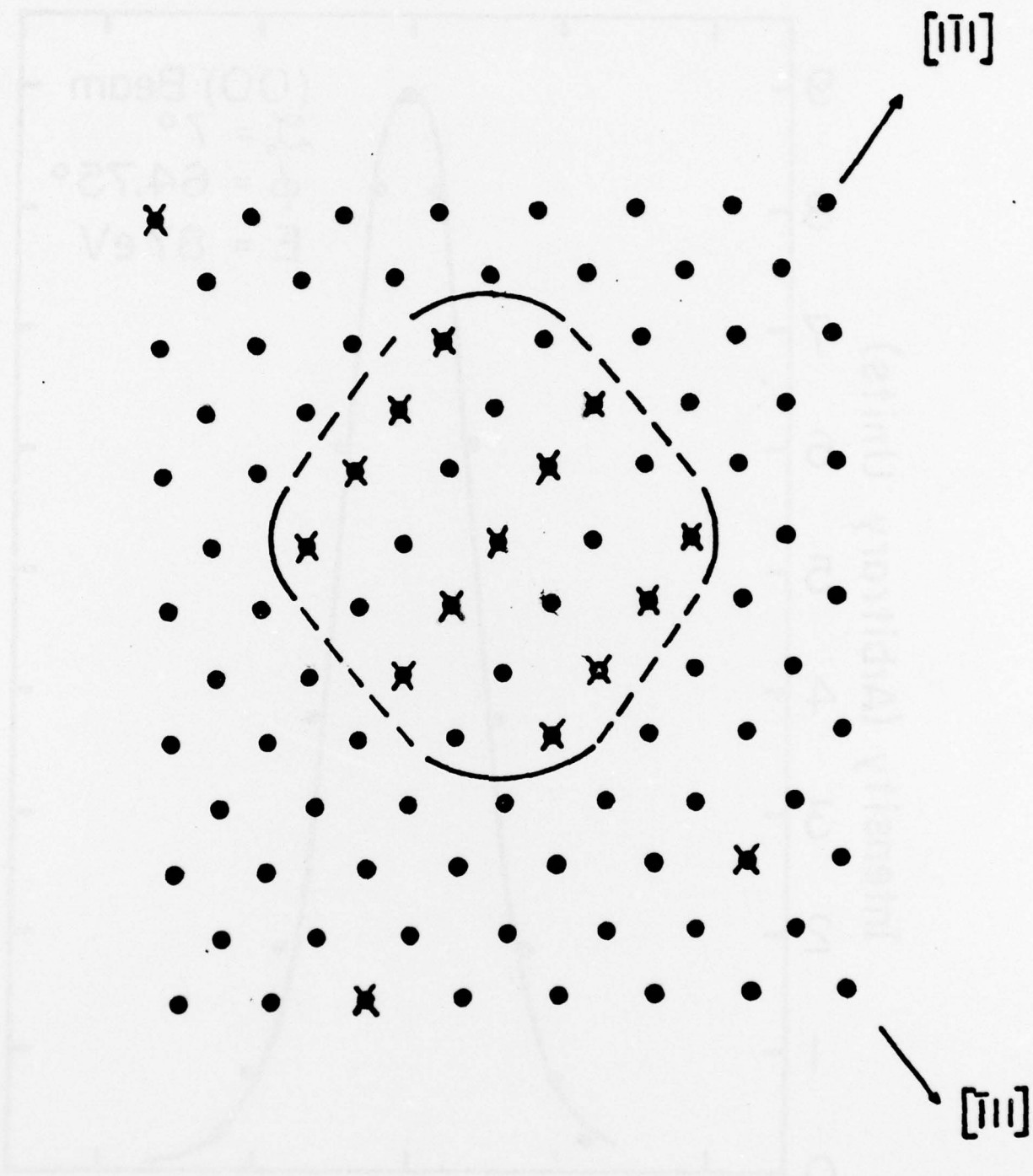
Figure 1

Figure 2

Figure 3

W(110)p(2X1)-O
(1/2,1/2)BEAM
E=52 eV
$\vartheta_0 = 0°$
$\phi = 35.25°$
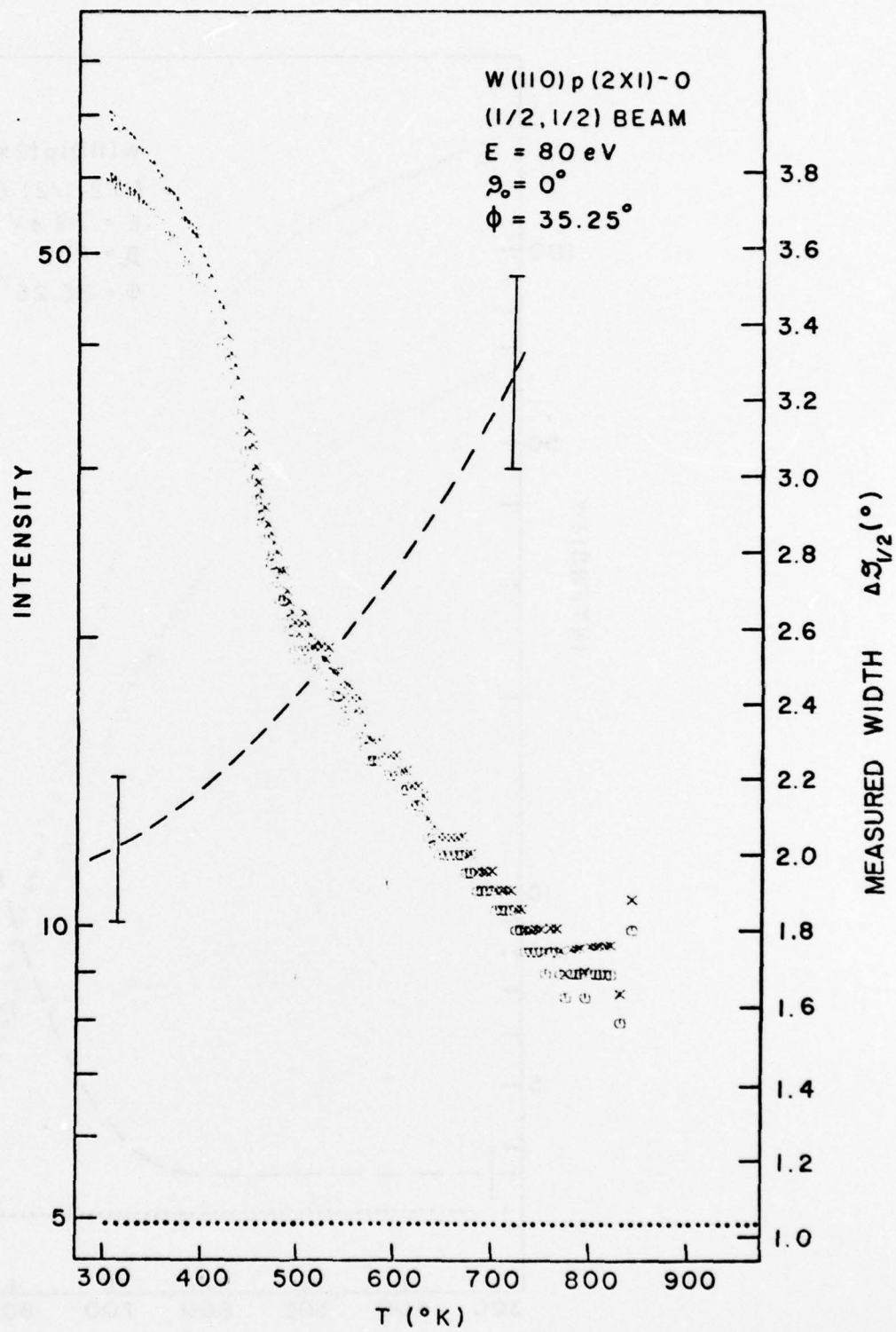
Figure 4

W(110)p(2X1)-O
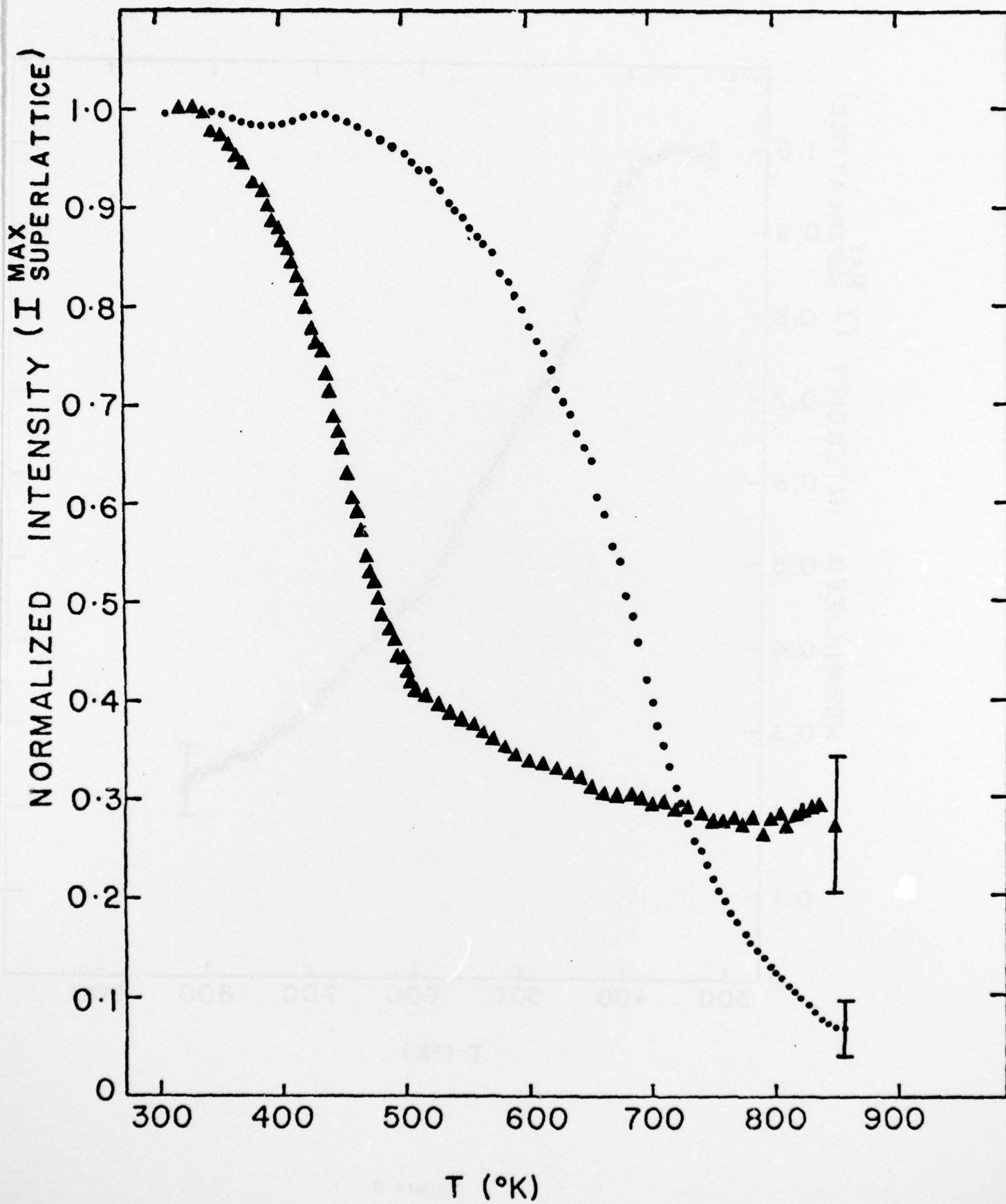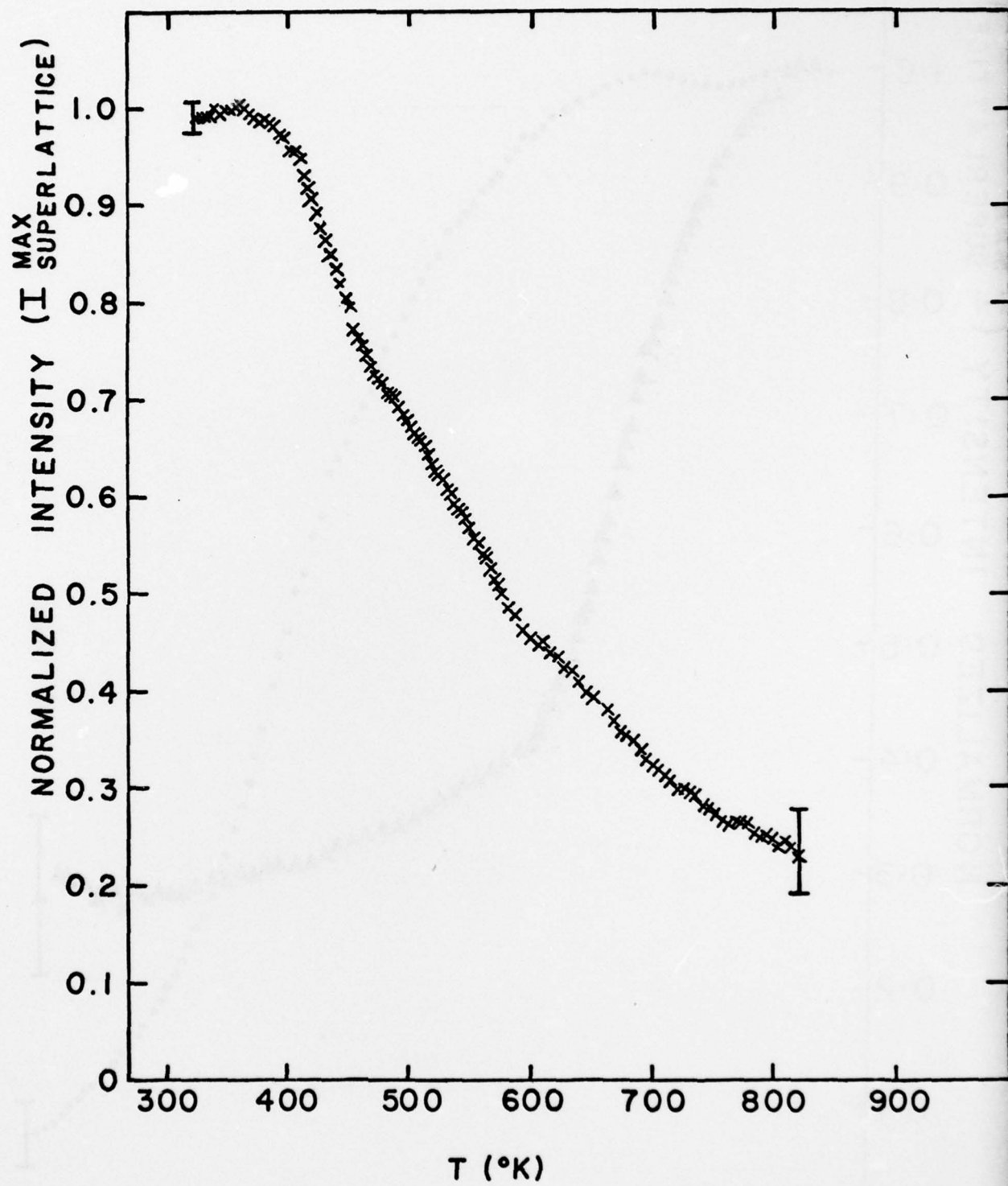(1/2,1/2) BEAM
E = 79 eV
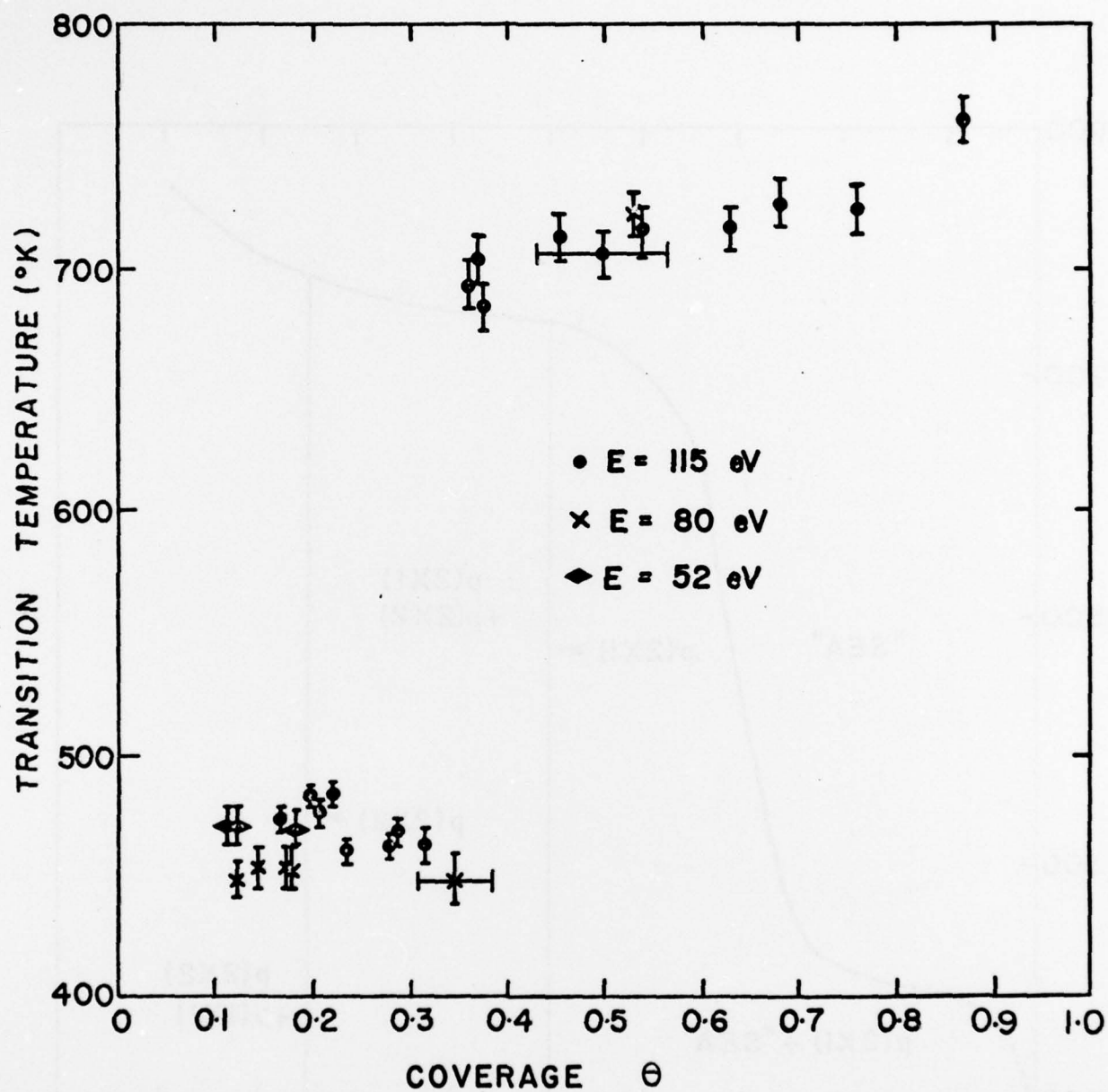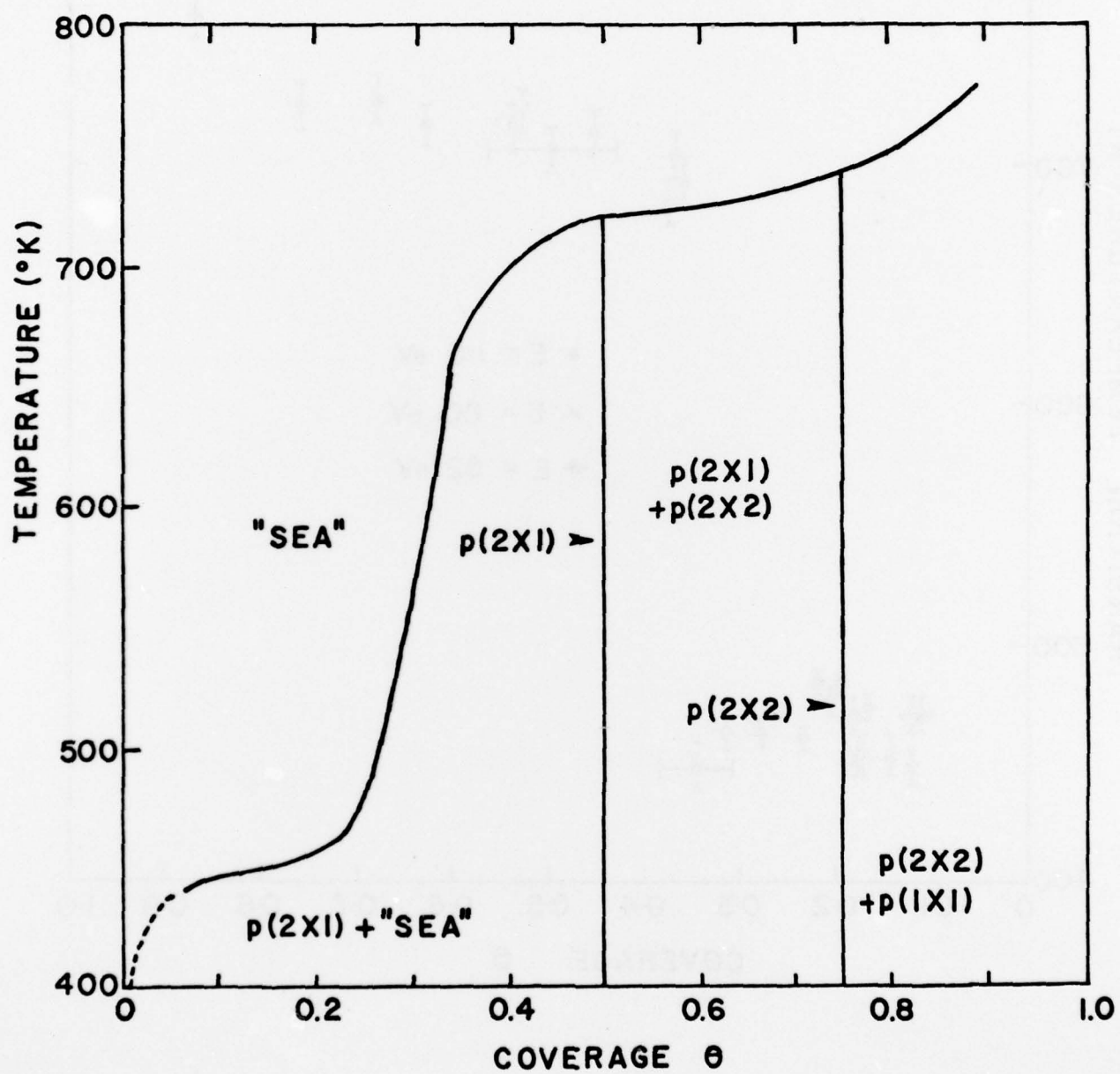$\vartheta_0 = 0°$
$\phi = 35.25°$
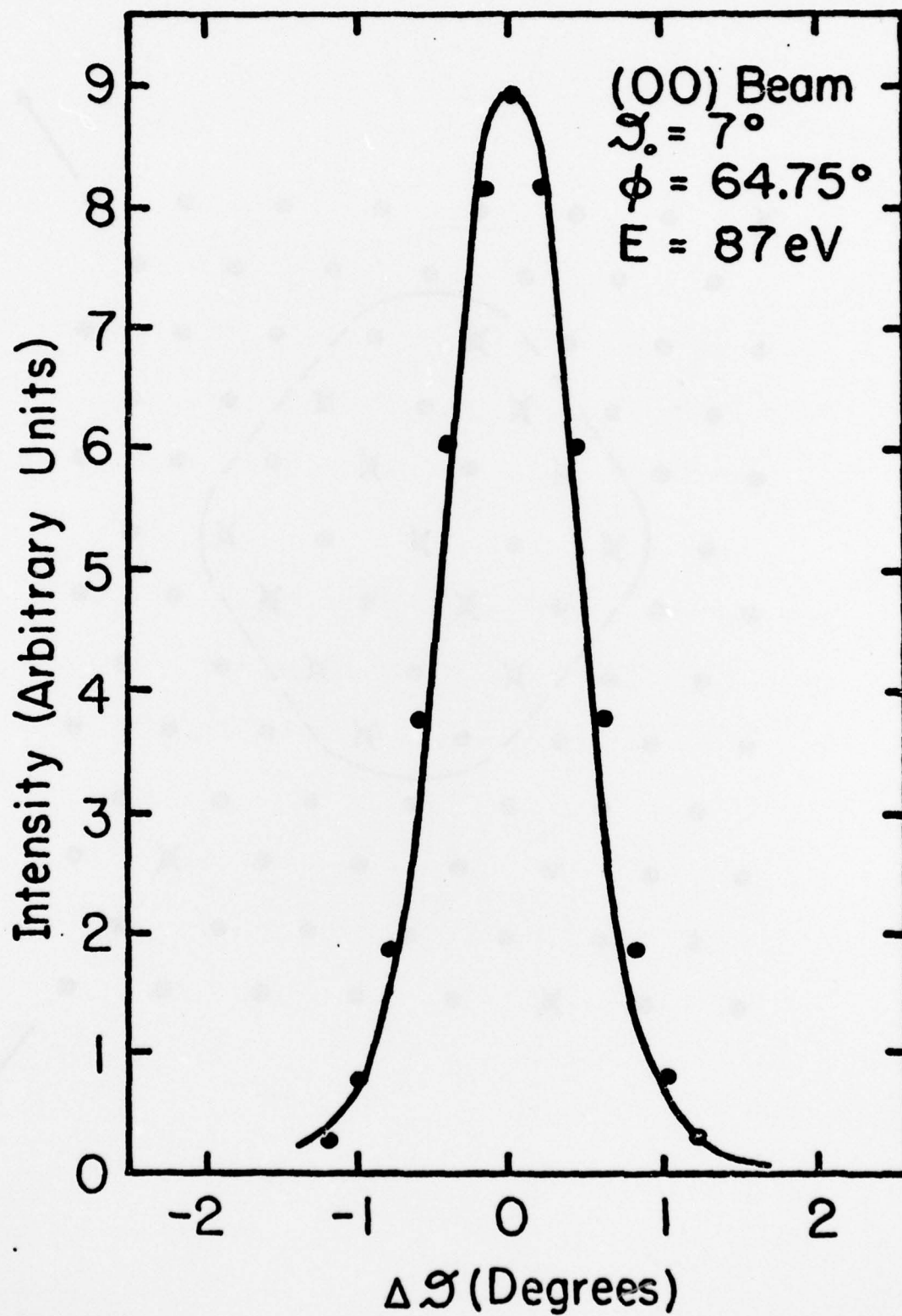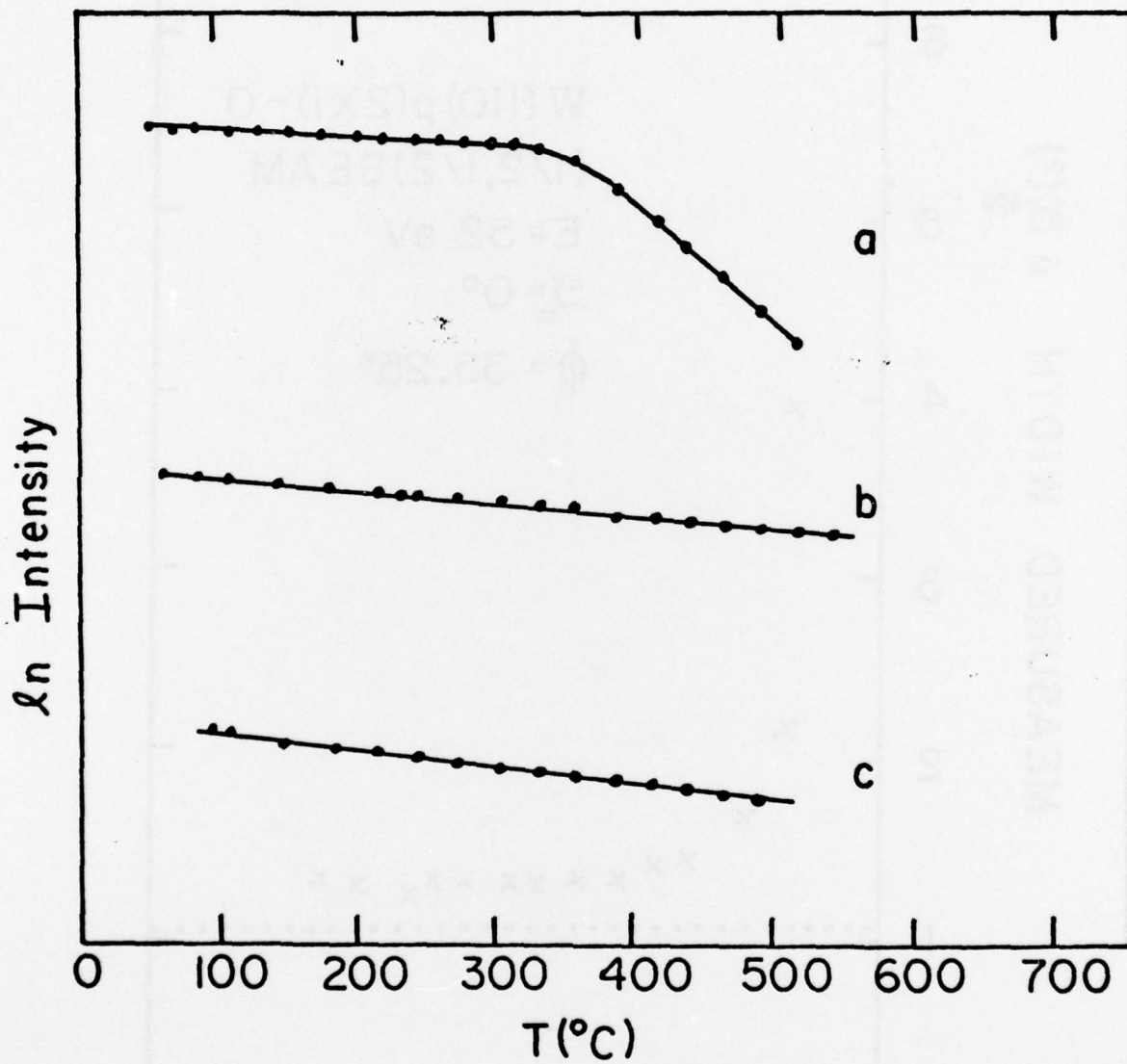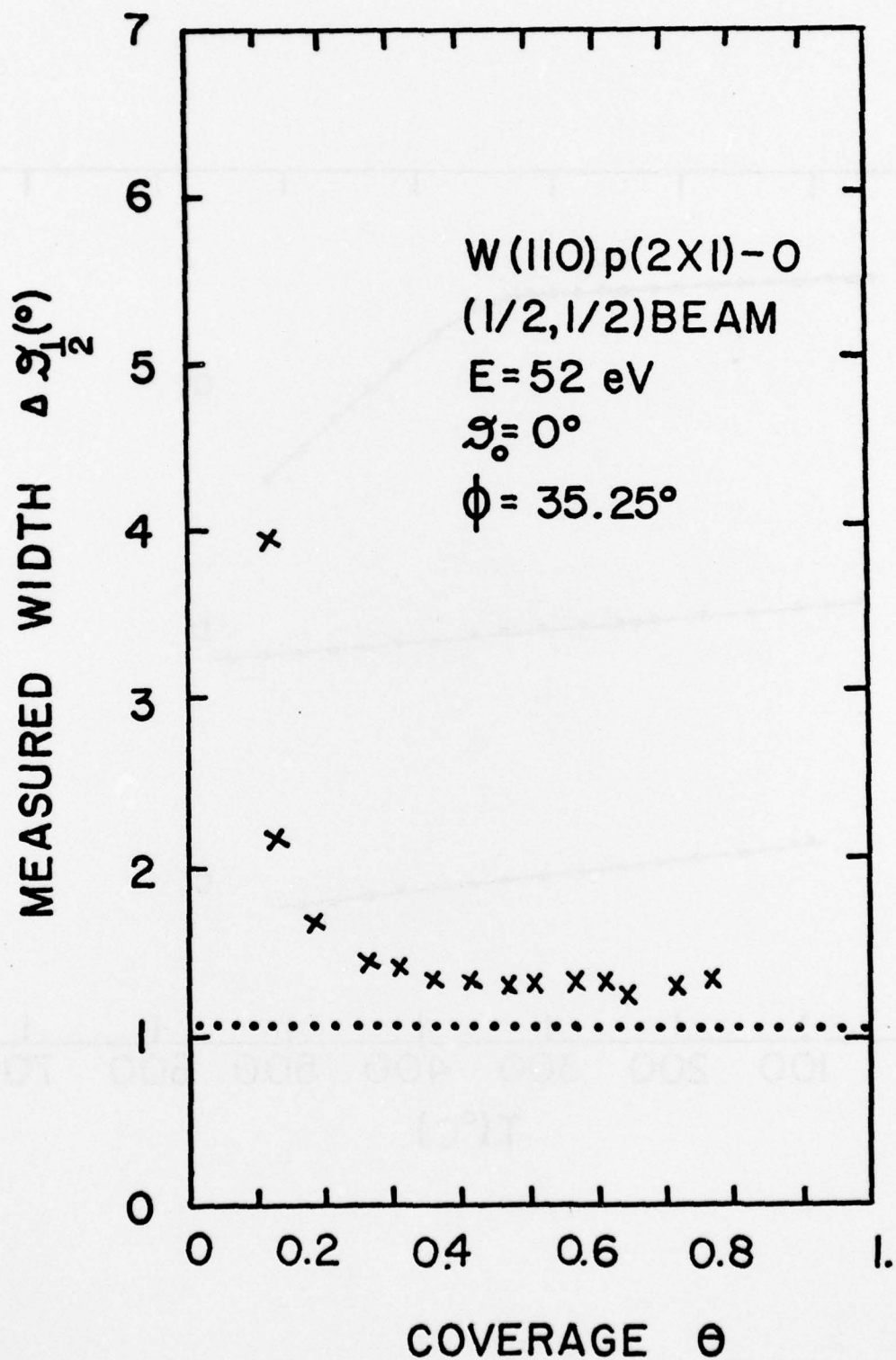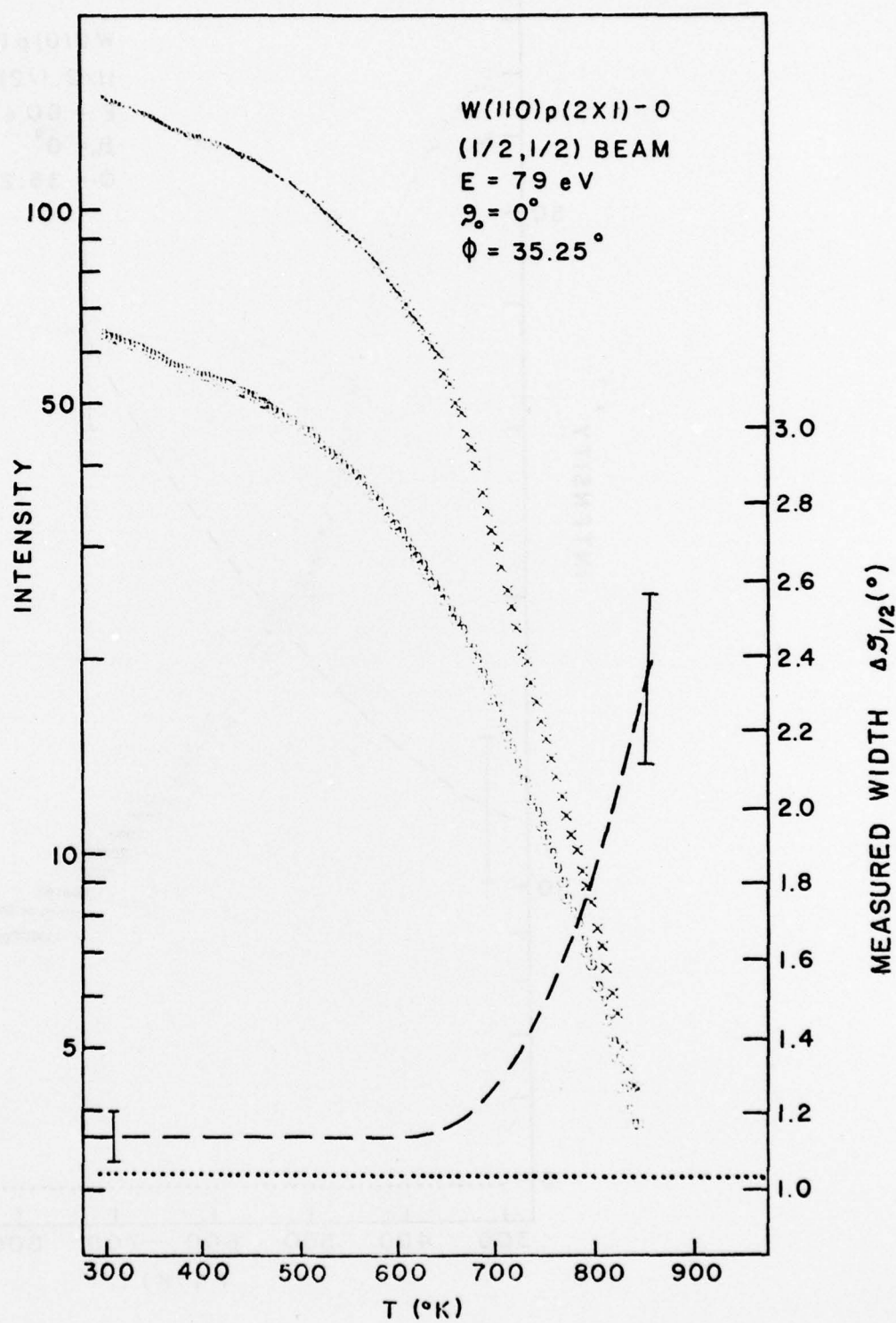
Figure 5

Figure 6

Figure 7

Figure 8

Figure 9

Figure 10a

Figure 10b

Figure 10c